

## Liquid Phase Deposition of TiO<sub>2</sub> Films for Electron Transport Layer of Perovskite Solar Cells

Ari Sulisty Rini<sup>1</sup>, Mahagi P. Deraf<sup>1</sup>, H. Yanuar<sup>1,\*</sup>, A.A. Umar<sup>2</sup>

<sup>1</sup> Department of Physics, FMIPA, Universitas Riau, 28293 Pekanbaru, Indonesia

<sup>2</sup> Institute of Microengineering and Nanoelectronics (IMEN), Universiti Kebangsaan Malaysia, Selangor, Bangi 43600, Malaysia

(Received 11 February 2020; revised manuscript received 15 June 2020; published online 25 June 2020)

The TiO<sub>2</sub> layer plays an important role in organic lead-halide perovskite solar cells (PSCs) as an electron transport layer as well as a blocking layer to prevent carrier recombination at the interface of fluorine-doped tin oxide (FTO) and a perovskite layer. TiO<sub>2</sub> thin film was successfully grown on FTO substrate using the liquid phase deposition method. In this work, TiO<sub>2</sub> layers were grown at a temperature of 50 °C. The first layer was grown for 2 h and the second layer was subsequently grown at different durations, i.e. 1, 2, 3, and 4 h. The optical, structural and morphological properties of the samples were characterized using UV-vis spectroscopy, XRD and FESEM/EDX, respectively. The TiO<sub>2</sub> thin film was then applied as an electron transport material (ETM) in the PSC *n-i-p* configuration. The UV-vis characterization results showed that the peak absorption spectrum of TiO<sub>2</sub> thin films occurred in the wavelength range of 300-450 nm for all samples. The XRD pattern indicated that the sample is anatase TiO<sub>2</sub> structure with the crystal orientation of (100), (004), (200) and (105) at the diffraction peak angle of  $2\theta$  25.50°, 37.92°, 48.04° and 54.84°, respectively. FESEM characterization showed that the TiO<sub>2</sub> nanostructure has a rod-like morphology. The PSC device fabricated utilizing the TiO<sub>2</sub> sample with a second layer grown for 2 h exhibits the highest power conversion efficiency of 0.23 %.

**Keywords:** TiO<sub>2</sub>, Liquid phase deposition, Electron transport material, FESEM, Perovskite solar cell.

DOI: [10.21272/jnep.12\(3\).03019](https://doi.org/10.21272/jnep.12(3).03019)

PACS numbers: 68.03.Fg, 81.15.Lm

### 1. INTRODUCTION

Perovskite solar cell (PSC) is a new generation of solar cells with promising performance as a result of excellent photophysical properties of the organo-lead halide perovskite materials. Initially, Miyasaka group applied CH<sub>3</sub>NH<sub>3</sub>PbI<sub>3</sub> organometal halide perovskite over TiO<sub>2</sub> as a substitute for light-absorbing material (dye) on DSSC and successfully achieved a cell efficiency of 3.8 % [1]. The device of PSCs has been developed based on the organic lead halides or mixed halides perovskites, e.g. CH<sub>3</sub>NH<sub>3</sub>PbI<sub>3</sub> or CH<sub>3</sub>NH<sub>3</sub>PbI<sub>3-x</sub>Cl<sub>x</sub> by another research group [2]. The power conversion efficiency (PCE) of PSCs has rapidly increased in the past few years from 9 to 22.1 % [3]. In general, PSCs consist of an electron transport layer (ETL), perovskite layer and hole transport layer (HTL). The high-performance PSCs commonly used TiO<sub>2</sub> thin film as ETL incorporating CH<sub>3</sub>NH<sub>3</sub>PbI<sub>3</sub> perovskite as a light absorber material [3].

There are two types of TiO<sub>2</sub> used as an ETL in PSC in terms of its porosity, i.e. compact and mesoporous TiO<sub>2</sub>. The compact TiO<sub>2</sub> layer will transfer photo-generated electrons from perovskite and, at the same time, it will act as a blocking layer to prevent direct contact between a hole and FTO which results in a decrease in cell efficiency [4]. The mesoporous TiO<sub>2</sub> is preferable to gain more contacts between ETL and the organic perovskite material [2]. The properties, structure and morphology of TiO<sub>2</sub> are strongly dependent on the preparation technique. The preparation method may influence the morphology and structure of TiO<sub>2</sub> film and indirectly influence the power conversion efficiency of solar cells. Several techniques have been reported to fabricate TiO<sub>2</sub>

as ETL, e.g. the hydrothermal method [5], screen-printing [6], DC magnetron sputtering, natural dropping [7] and sol-gel followed by spin-coating [8]. In many cases, those methods required expensive equipment and complicated procedures to obtain a required nanostructure of TiO<sub>2</sub>. The liquid phase deposition (LPD) method is a simple wet-chemical process to grow metal oxide thin film. The liquid phase deposition method has the advantage that can be carried out under atmospheric conditions at room temperature without using any special equipment [9]. The LPD can be done by reacting metal-fluoro complex with fluor anion scavenger of boric acid [10]. In this paper, the LPD technique has been employed to fabricate rod-like TiO<sub>2</sub> nanostructure without any directing agent. TiO<sub>2</sub> thin layers were fabricated in various growth times and then applied as ETL in PSC. The effect of variation in growth time on the optical properties, morphology, structure, and efficiency of PSC was then analyzed and discussed.

### 2. EXPERIMENTAL

#### 2.1 Material and Method

Ammonium hexafluortitanate ((NH<sub>4</sub>)<sub>2</sub>TiF<sub>6</sub>) (AHT), boric acid (H<sub>3</sub>BO<sub>3</sub>), lead (II) oxide (PbI<sub>2</sub>), poly[bis(4-phenyl)(2,4,6-trimethylphenyl)amine] and fluorine-doped tin oxide (FTO) glass were purchased from Sigma Aldrich and methylammonium iodide ((CH<sub>3</sub>NH<sub>3</sub>)I<sub>2</sub>) was supplied from Dyesol Ltd. Australia. (NH<sub>4</sub>)<sub>2</sub>TiF<sub>6</sub> and H<sub>3</sub>BO<sub>3</sub> were used as precursors and anion scavenger, respectively, for the synthesis of TiO<sub>2</sub>. PbI<sub>2</sub> and methylammonium iodide were used as a starting material for

\* [yanuar.hamzah@gmail.com](mailto:yanuar.hamzah@gmail.com)

synthesis of organo-metal halide  $\text{CH}_3\text{NH}_3\text{PbI}_3$  perovskite. Poly[bis(4-phenyl) (2,4,6-trimethylphenyl)amine] (PTAA) was used for the hole transport material (HTM), while dimethylformamide was used as solvent. First, the FTO substrate was cut and cleaned by consecutive ultrasonication in acetone, ethanol and deionized water. The preparation procedure of  $\text{TiO}_2$  thin films referred to the method published previously [9]. Typically, 5 ml of 0.1 M  $(\text{NH}_4)_2\text{TiF}_6$  and 5 ml of 0.2 M  $\text{H}_3\text{BO}_3$  aqueous solution were mixed and then used as a growth solution. The FTO substrate was placed vertically in the growth solution at a temperature of 50 °C. The  $\text{TiO}_2$  films were grown twice with the same growth condition. For all samples, the first layer was grown for 2 h. The second layers were grown at different times, i.e. 1, 2, 3 and 4 h. The prepared thin film of  $\text{TiO}_2$  was then taken out of the solution, washed with an abundant of DI-water, dried with nitrogen flow and annealed at 400 °C for 30 min. The samples were named according to their first ( $x$ ) and second ( $y$ ) growth time in hours, i.e.  $\text{T}x\text{-}y$ . The organic perovskite coating was done by the two-step method. In the first step, 400 mg/ml of  $\text{PbI}_2$  in dimethylformamide was spin-coated onto the  $\text{TiO}_2$  layer at a speed of 3000 rpm for 10 s. This layer was then annealed at 100 °C for 5 min. In the second step, 40 mg/ml of methylammonium iodide (MAI) in 2-propanol was spin-coated at a speed of 3000 rpm for 10 s. The samples were then annealed at 100 °C for 30 min. The HTM layer is prepared by spin-coating 20 mg/ml PTAA on the perovskite layer. Samples were annealed at 100 °C for 10 min. The final step was fabricating metal electrodes by sputtering the platinum metal over the sample with an active area of 0.23  $\text{cm}^2$ .

## 2.2 Characterization

Optical properties of thin films were characterized using Hitachi U-3900H UV-vis spectroscopy (Lambda 900 Perkin-Elmer) and surface morphology was characterized by Field-Effect Electron Scanning Microscopy (FESEM) (Zeiss SUPRA 55VP). The structure and crystallinity of the samples were characterized using X-ray diffraction (BRUKER D8 Advance) with  $\text{CuK}\alpha$  radiation ( $\lambda = 0.154$  nm) and a scan step of 2°/min. The PSC performance utilizing the samples with various growth times was recorded by high-voltage source (Keithley model 237). The current-voltage measurements were carried out under AM 1.5 simulated light illumination with an intensity of 100  $\text{mW}/\text{cm}^2$ .

## 3. RESULTS AND DISCUSSION

Fig. 1 shows the UV-visible optical absorption spectrum of  $\text{TiO}_2$  sample grown using a liquid phase deposition method with different growth times. The UV-vis absorption spectrum of the sample shows the dominant absorption peak in the UV region. The absorption peak occurs in the range of wavelengths 300-350 nm [11]. This result was also observed in [12]. The sample prepared without the second layer (T2-0) possesses the lowest absorption peak in the UV light range, while the highest absorption peak belongs to the sample prepared for 3 h of second-growth time (T2-3). It is also obvious that the absorption area varies with the

growth time of the secondary layer. The sample prepared for 4 h of the second layer (T2-4) demonstrates the largest absorption area, and the sample without the secondary layer (T2-0) has the smallest absorption area. The peak of UV-vis absorption of  $\text{TiO}_2$  layer that grew more than 1 layer was observed to shift towards larger wavelengths and was at a wavelength of around 350-380 nm (near visible light).

The magnitude of the energy band gap of all the samples was calculated. The UV-vis absorption spectrum produced by semiconductor samples provides a correlation between the absorbance and the photon energy needed to excite the electrons from the valence band to the conduction band. The relationship between the photon beam energy of excitation and the band gap energy (band gap,  $E_g$ ) is given by the Tauc equation:

$$(Ah\nu)^n = A \cdot (h\nu - E_g). \quad (1)$$

The power of  $n$  for indirect energy gap is equal to 1/2 and 2 for direct energy gap. The energy of the optical band gap  $E_g$  for  $\text{TiO}_2$  is obtained by extrapolating the curve  $h\nu$  vs  $(ah\nu)^{1/2}$ . The intercept of the straight line for the  $x$ -axis is defined as the value of  $E_g$  (Fig. 1b). The value of energy gap for all the samples is listed in Table 1.

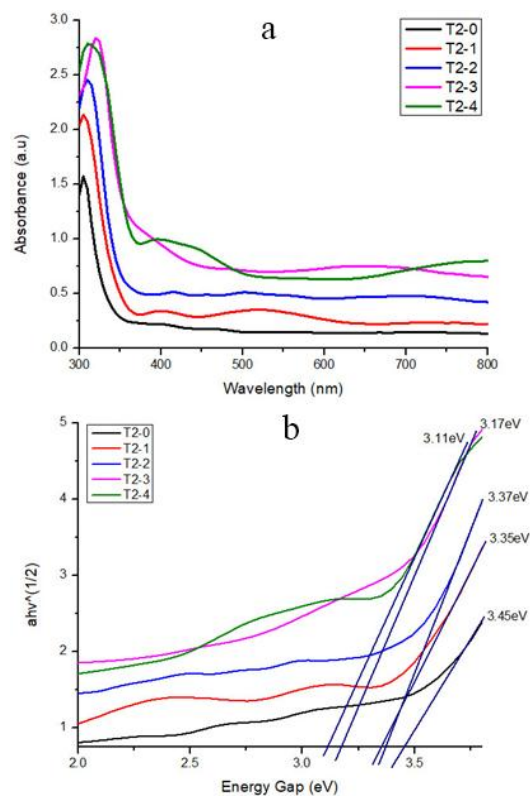
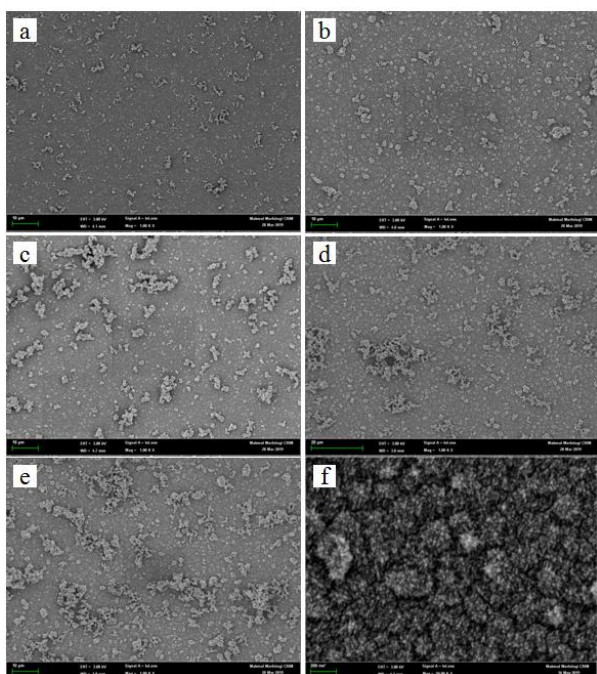


Fig. 1 – UV-vis spectra (a) and energy band gap calculation (b)

Table 1 – Energy band gap of  $\text{TiO}_2$  at different growth times

No	Sample	Energy band gap (eV)
1	T2-0	3.45
2	T2-1	3.35
3	T2-2	3.37
4	T2-3	3.17
5	T2-4	3.11

Fig. 2a, f show the top view FESEM images of TiO<sub>2</sub> samples grown for 2 h (T2-0) as a basis layer with 1.000 and 50.000 times magnification, respectively. Fig. 2b-e are FESEM images of the sample subsequently grown for the second layer for 1, 2, 3 and 4 h at a temperature of 50 °C. It is obviously noticed that the morphological shape of the sample changes with growth time. It can be seen that for 2 h of growth time, the TiO<sub>2</sub> rod-like structure has been obtained. This result agrees well with the morphology of TiO<sub>2</sub> film prepared by LPD by Umar and his group [9]. As the first layer subjected to the second-growth process, it can be seen that the precursor initiates another structure on the surface [12]. As the growth time for the second process increases, a bigger grain size was obtained. FESEM images of as-deposited films observed the existence of cracks. Cracks generally occur due to the intrinsic high surface tension of the TiO<sub>2</sub> layer [9]. The presence of the crack might increase the porosity of the film.

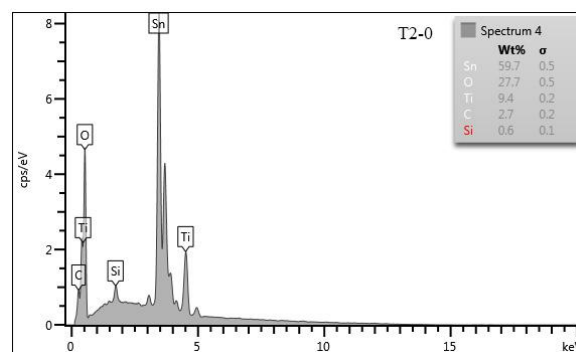


**Fig. 2** – FESEM image of the samples: T2-0 (a), T2-1 (b), T2-2 (c), T2-3 (d), T2-4 (e), T2-0 (f) with magnification of 50.000x

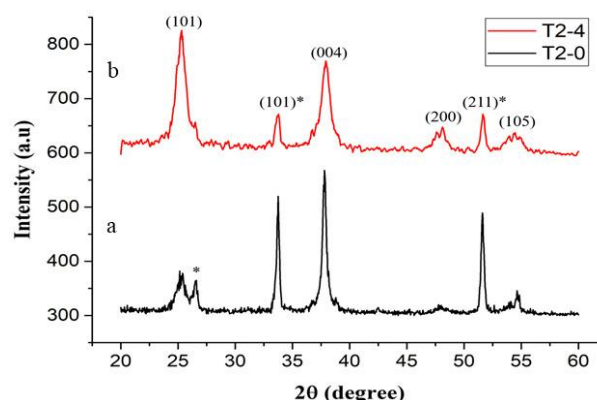
The EDX spectrum of sample T2-0 is shown in Fig. 3. The picture also displays the percentage of the weight of the constituent atoms contained in the sample. Based on EDX data, there are elements Sn, C and Si in the sample. The Ti and O content in TiO<sub>2</sub> sample with the growth time of 2 h (T2-0) are 9.4 and 27.77 (wt. %), respectively. The appearance of Sn element comes from the FTO substrate due to the fact that T2-0 is the sample with the thinnest layer, with a percentage of atomic weight of 59.7 %. In addition, there are also carbon and silica elements derived from combustion (annealing), each of which has a percentage of atomic weight of 2.7 % and 0.6 %, respectively.

Fig. 4 shows the XRD spectra of two selected samples, i.e. single layer and double layer samples, namely T2-0 and T2-4, respectively. It indicates that sample T2-0 (single layer) still reveals strong diffraction from FTO. After the addition of the second layer grown for

4 h, that is sample T2-4, strong diffraction from (101) plane was observed, which agrees with the JCPDS card file no. 96-900-9087 [13].



**Fig. 3** – EDX spectrum of TiO<sub>2</sub> with growth time of 2 h



**Fig. 4** – XRD spectrum of TiO<sub>2</sub> with growth time of 2 h

**Table 2** – Material properties used in this study

Sample	$\beta$ (°)	FWHM (rad.)	Crystallite size (nm)
T2-0	37.92	0.464	29.56
T2-4	38.20	0.942	14.56

Thus, X-ray diffraction peaks at 25.50°, 37.92°, 48.04°, and 54.84° correspond to (101), (004), (200), and (211) plane of anatase TiO<sub>2</sub>, respectively. The calculated lattice parameters of anatase TiO<sub>2</sub> are  $a = 0.37796$  nm and  $c = 0.94858$  nm. Anatase-TiO<sub>2</sub> is preferable to be applied as an electron transport layer in PSC due to its high photoactivity properties. The crystalline size can be calculated from the FWHM value of X-ray diffraction peak using the Scherrer's formula. The FWHM values of (400) plane of T2-0 and T2-4 samples were obtained using the Origin Pro 2016. FWHM values and calculated crystallite sizes are listed in Table 2. According to XRD spectra, T2-0 sample has a large crystallite size compared to the T2-4 sample in [400] direction. Constructive interference that occurs due to the crystalline plane will be higher if the crystalline size is also large.

Fig. 5a, b demonstrate the  $J$ - $V$  curve of the fabricated PSC device using TiO<sub>2</sub> film grown with different growth times in dark and under 100 mW/m<sup>2</sup> illumination, respectively. In dark conditions, the  $J$ - $V$  curves show typical semiconductor diode characteristics. The smaller the potential difference required by the electron to be excited (a rapid increase in current), the better the solar cell will work.

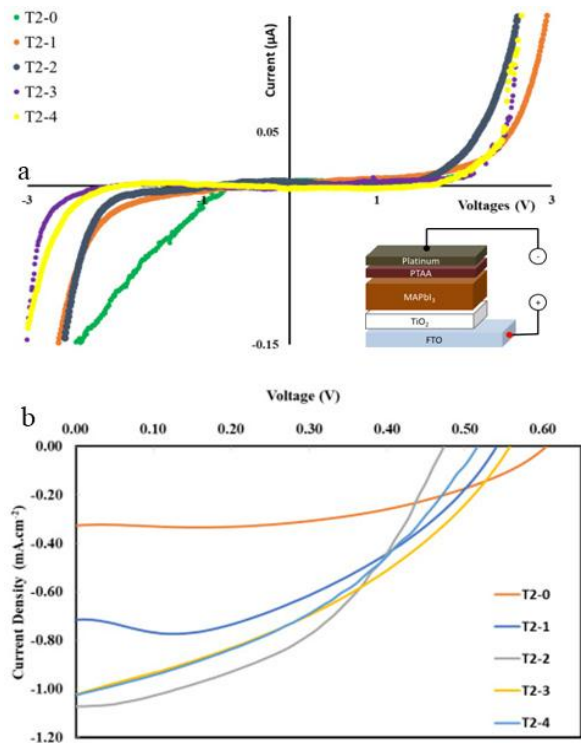


**Fig. 5** –  $J$ - $V$  curve (a) in dark and cell configuration for the PSC performance measurement (insert) and (b) under illumination of  $100 \text{ mW/m}^2$  for the PSC with different growth time of  $\text{TiO}_2$

The thickness of the ETM was found to influence the PSC performance, as expected. We assumed that  $\text{TiO}_2$  electron selective growth time is related to their layer thickness. Table 3 summarizes the photovoltaic properties of PSC utilizing LPD prepared  $\text{TiO}_2$  samples based on the  $J$ - $V$  curves from Fig. 5b. Sample with a

single  $\text{TiO}_2$  layer (T2-0) has the highest open-circuit voltage ( $V_{oc}$ ) but the lowest short-current density ( $J_{sc}$ ) and the lowest efficiency, i.e. 0.1 %.

Addition of the second layer grown for 1 h has significantly increased the efficiency up to 0.19 %. The sample prepared by double layer deposition for 2 and 2 h (T2-2) possesses the lowest  $V_{oc}$  but the highest  $I_{sc}$  and resulted in the highest solar cell efficiency, i.e. 0.23 %.

**Table 3** – Measurement data and calculation of PSC based on  $\text{TiO}_2$  with variations in growth temperature

Sample	$V_{oc}$ (V)	$J_{sc}$ ( $\text{mA/cm}^2$ )	FF	$\eta$ (%)
T2-0	0.56	0.329	0.526	0.10
T2-1	0.54	0.720	0.483	0.19
T2-2	0.47	1.071	0.453	0.23
T2-3	0.55	1.033	0.377	0.22
T2-4	0.51	1.036	0.395	0.21

#### 4. CONCLUSIONS

In this work,  $\text{TiO}_2$  thin films were successfully grown on FTO by using the liquid-phase deposition method with various growth times and were applied as an electron transport material to the PSC device. It was observed that the morphology and the optical absorbance of the samples were influenced by the  $\text{TiO}_2$  growth time. The highest  $J_{sc}$  of 1.071 and  $\eta$  of 0.23 % were obtained for PSC utilizing the sample grown at  $50^\circ\text{C}$  for 2 h each.

#### ACKNOWLEDGEMENTS

This work was financially supported by LPPM, Universitas Riau under DIPA Fund. The authors also thank CRIM and IMEN UKM for the facilities during preparation and characterization.

#### REFERENCES

1. A. Kojima, K. Teshima, Y. Shirai, T. Miyasaka, *J. Am. Chem. Soc.* **131**, 6050 (2009).
2. Hui-Seon Kim, Chang-Ryul Lee, Jeong-Hyeok Im, Ki-Beom Lee, Thomas Moehl, Arianna Marchioro, Soo-Jin Moon, Robin Humphry-Baker, Jun-Ho Yum, Jacques E. Moser, Michael Grätzel, Nam-Gyu Park, *Sci. Rep.* **2** No 591, 1 (2012).
3. D. Zhou, T. Zhou, Y. Tian, X. Zhu, and Y. Tu, *J. Nanomater.* **2018**, 8148072 (2018).
4. Y. Rong, Y. Hu, A. Mei, H. Tan, M.I. Saidaminov, S. Il Seok, M.D. McGehee, E.H. Sargent, H. Han, *Science* **361**, eaat. 8235 (2018).
5. M. Giannouli, *Int. J. Photoenergy* **2013**, 612095 (2013).
6. P. Jiang, T.W. Jones, N.W. Duffy, K.F. Anderson, R. Bennett, M. Grigore, P. Marvig, Y. Xiong, T. Liu, Y. Sheng, Li Hong, X. Hou, M. Duan, Y. Hu, Y. Rong, G.J. Wilson, H. Han, *Carbon* **129**, 830 (2018).
7. Y. Yamashita, K. Ishiguro, D. Nakai, M. Fuji, *Adv. Powder Technol.* **29**, 2521 (2018).
8. J. Qin, Z. Zhang, W. Shi, Y. Liu, H. Gao, Y. Mao, *Nanoscale Res. Lett.* **12**, 640 (2017).
9. A.A. Umar, M.Y.A. Rahman, S.K.M. Saad, M.M. Salleh, M. Oyama, *Appl. Surf. Sci.* **270**, 109 (2013).
10. A.A. Umar, S.K.M. Saad, M.I. Ali Umar, M.Y.A. Rahman, M. Oyama, *Opt. Mater. (Amst.)* **75**, 390 (2018).
11. P. Magalhães, L. Andrade, O. C. Nunes, A. Mendes, *Rev. Adv. Mater. Sci.* **51**, 91 (2017).
12. A.S. Sulaiman, M.Y.A. Rahman, A.A. Umar, M.M. Salleh, *Russ. J. Electrochem.* **54**, 56 (2018).
13. S.K.M. Saad, A.A. Umar, S. Nafisah, M.M. Salleh, and B.Y. Majlis, *Proceedings – RSM 2013: IEEE Regional Symposium on Micro and Nano Electronics*, 402 (2013).
14. M. Salado, L. Calio, L. Contreras-Bernal, J. Idígoras, J.A. Anta, S. Ahmad, S. Kazim, *Materials (Basel)* **11**, 1073 (2018).
15. Q. Gao, S. Yang, L. Lei, S. Zhang, Q. Cao, J. Xie, J. Li, Y. Liu, *Chem. Lett.* **44**, 624 (2015).

## Осадження рідкої фази плівок TiO<sub>2</sub> для електронно-транспортного шару перовскітних сонячних елементів

Ari Sulistyono Rini<sup>1</sup>, Mahagi P. Deraf<sup>1</sup>, H. Yanuar<sup>1</sup>, A.A. Umar<sup>2</sup>

<sup>1</sup> Department of Physics, FMIPA, Universitas Riau, 28293 Pekanbaru, Indonesia

<sup>2</sup> Institute of Microengineering and Nanoelectronics (IMEN), Universiti Kebangsaan Malaysia, Selangor, Bangi 43600, Malaysia

Шар TiO<sub>2</sub> відіграє важливу роль в органічних свинцево-галогенідних перовскітних сонячних елементах (PSCs) як електронно-транспортний шар, а також як блокуючий шар для запобігання рекомбінації носіїв на межі поділу легованого фтором оксиду олова (FTO) та перовскітного шару. Тонку плівку TiO<sub>2</sub> успішно вирощували на підкладці FTO методом осадження рідкої фази. У цій роботі шари TiO<sub>2</sub> вирощували в два заходи при температурі 50 °C. Перший шар вирощували протягом 2 год, а другий шар згодом вирощували з різною тривалістю, а саме протягом 1, 2, 3 та 4 год. Оптичні, структурні та морфологічні властивості зразків характеризували відповідно за допомогою УФ-спектроскопії, XRD та FESEM/EDX. Потім тонку плівку TiO<sub>2</sub> застосовували як електронно-транспортний матеріал (ETM) у PSC з конфігурацією *n-i-p*. Результати УФ-спектроскопії показали, що спектр максимального поглинання тонких плівок TiO<sub>2</sub> відповідає діапазону довжин хвиль 300-450 нм для усіх зразків. На дифрактограмі виявлено, що зразок є структурою анатазу TiO<sub>2</sub> з кристалічною орієнтацією (100), (004), (200) і (105) при кутах пікової дифракції  $2\theta$ , рівними відповідно 25,50°; 37,92°; 48,04° і 54,84°. FESEM характеристика показала, що наноструктура TiO<sub>2</sub> має стрижнеподібну морфологію. Пристрій PSC, виготовлений з використанням зразка TiO<sub>2</sub> з другим шаром, вирощеним протягом 2 год, демонструє найвищу ефективність перетворення потужності, рівну 0,23 %.

**Ключові слова:** TiO<sub>2</sub>, Осадження рідкої фази, Електронно-транспортний матеріал, FESEM, Перовскітні сонячні елементи.